Ruthenium complex hydride catalysts as a platform for ammonia synthesis

Qianru Wang,[1,2] Jianping Guo,[1] Ping Chen[1,3]*

[1]Dalian National Laboratory for Clean Energy, Dalian Institute of Chemical Physics, Chinese Academy of Sciences, Dalian, China.
[2]University of Chinese Academy of Sciences, Beijing, China.
[3]State Key Laboratory of Catalysis, Dalian, China.
*Correspondence to: pchen@dicp.ac.cn.

Abstract

Mild-condition ammonia synthesis from N_2 and H_2 is a long-sought-after scientific goal and a practical need, especially for the intensively pursued "Green Ammonia" production using renewable H_2. Under this context, there have been growing interests in the development of new catalysts for effectively catalyzing N_2+H_2 to NH_3. Particular attention has been given to Ru-based catalysts because they are well known to be more active at lower temperatures and pressures than non-noble-metal based catalysts. Here, we demonstrate that a series of Ru complex hydrides $A_n[RuH_m]$, where A is alkali or alkaline earth metal, n= 2, 3 or 4 and m = 6 or 7, exhibit universal and high catalytic activities that far exceed the benchmark Ru metal catalysts under mild conditions. Detailed investigations on the ternary Ru complex hydride catalytic system disclose that the kinetic behaviors depend strongly on the identity of alkali or alkaline earth metal cations. In clear contrast to the closed packed Ru metal catalyst, the unique configuration and synergized scenario of the Ru complex hydride center prefer a non-dissociative mechanism for N_2 activation and hydrogenation, which provides a new platform for the design and development of efficient NH_3 synthesis catalysts.

Introduction

Ammonia, as one of the most important chemicals and carbon-free energy carriers, has a worldwide production of ~180 million tons per year, and is mainly produced by the industrial Haber-Bosch (HB) process with Fe-based catalyst [1].

Currently, the large-scale and centralized HB process accounts for nearly 2% of the world's consumption of fossil fuels and consequently over 1% of the global anthropogenic CO_2 emissions, mainly due to the fact it employs fossil-fuel sourced H_2 and requires harsh operating conditions (400-500 ºC,100-300 bar) [2]. Therefore, there is an imperative to decarbonize ammonia industry and reduce the energy cost, which spurs recent interest in finding sustainable alternatives. Establishing a CO_2-free, flexible-scale, distributed process capable of coping with the intermittent and variable renewable energy supplies may open a range of opportunities for the second ammonia revolution [3].

As the electric power generated from renewable energy sources becomes more technically and economically viable, nowadays much efforts have been placed on the electrolysis Haber-Bosch process (*e*HB), where renewable electricity is used to electrolyze H_2O to produce H_2, separate N_2 from air and power the N_2+H_2 to NH_3, etc [4-5]. To improve its compatibility with the renewable electricity as well as to reduce the energy cost, the *e*HB process generally requires an active catalyst that can operate at lower pressures (< 50 bar) and lower temperatures (< 673 K) [6]. It is well known that Ru is more active than Fe under milder reaction conditions. However, the high kinetic barrier for N_2 direct dissociation and the severe poisoning effect of hydrogen on Ru metal surface render efficient NH_3 synthesis under lower temperatures (< 623 K) unattainable [7]. Under this scenario, new Ru based catalytic systems have been intensively explored in recent years, aiming at facilitating ammonia synthesis under mild conditions. For example, advanced materials such as electrides [8], hydrides [9-11], amides [12-13], reducible metal oxides [14-15] have been developed as functional supports of Ru metal catalysts, which can strongly enrich the electron density of Ru and thus promote the cleavage of N_2 to form NH_3 on Ru metal surface under pressures below 5 MPa and temperatures below 673 K.

We recently reported that ruthenium complex hydrides Li_4RuH_6 and Ba_2RuH_6, as an entirely new class of ammonia synthesis catalysts, performs extraordinarily well under more benign conditions (< 573 K, 1 MPa). The key to achieve efficient

ammonia synthesis under mild conditions lies in the unique configuration and function mechanism of the complex hydride center, which is clearly different from the Ru metal based catalysts. For ternary complex hydride catalyst Li_4RuH_6 or Ba_2RuH_6, Ru is in an ionic state coordinated with Li(Ba) and H, and N_2 undergoes non-dissociative hydrogenolysis over electron-rich $[RuH_6]^{4-}$ complex center with the aid of surrounding Li/Ba cations and hydridic hydrogens (H^-). Besides Li_4RuH_6 and Ba_2RuH_6, there are abundant solid-state complex hydrides composed of various transition metal (TM) elements and alkali or alkali-earth (A) elements [16]. In the simplest compositions of these systems, all hydrogen atoms are bonded to the TM center giving the general chemical formula $A_n^{\delta+}[TMH_m]^{\delta-}$ (m, n, δ = 1, 2, 3 …), where the homoleptic, anionic TM-hydrido complexes $[TMH_m]^{\delta-}$ are stabilized by charge transfer from the surrounding alkali or alkali earth cations $A^{\delta+}$. In homogeneous N_2 fixation, it is well known that molecular TM hydride complexes, with the hydride ligands being the source of both electron and proton, serves as a common platform for N_2 activation [17-18]. In analogy to the configuration of molecular TM hydride complexes, the solid-state TM complex hydrides also show a lack of TM-TM bond and a plenty of electron-rich hydrido hydrogens, which might create a suitable structure and reacting environment for non-dissociative N_2 activation and hydrogenation. In this work, ternary Ru complex hydride series, as one of the most well-characterized complex hydrides, was chosen as the typical representative to demonstrate the potency of complex hydrides in N_2 fixation.

The open question here is whether other alkali or alkaline earth metal based ruthenium hydrides, such as Ca_2RuH_6, Na_4RuH_6 and K_3RuH_7, would resemble Li_4RuH_6 or Ba_2RuH_6 to achieve high catalytic performance for mild-condition ammonia synthesis, and whether a general approach for effective catalysis can be derived from the understanding of the cooperation and synergy of the Ru complex hydride center. This report starts with a systematical analysis on the structural and electronic configurations as well as the thermodynamic properties of the ternary Ru complex hydride series. Then, we demonstrate that these ternary complex hydrides

are chemically stable under ammonia synthesis conditions, and all studied complex hydrides can show superior performances under mild conditions when the ternary hydride sites are effectively exposed. Furthermore, the kinetic behaviors of these ternary complex hydride catalysts vary depending on the identity of the alkali or alkaline earth cations, but all of them show a balanced affinity towards H_2 and NH_3, which provides a favorable scenario for effective ammonia synthesis. The catalytic reaction mechanism derived from the ternary ruthenium complex hydride catalysts are clearly different from that of the Ru metal based catalysts, and therefore provides a new strategy for the design and development of efficient NH_3 synthesis catalysts.

Results and discussion

Ternary ruthenium complex hydrides have the general composition of $A_n^{\delta+}[RuH_m]^{\delta-}$ (A=Li, Na, K, Ca or Ba etc.; m=6 or 7; n=2, 3 or 4; δ=1, 2 or 3), where the $[RuH_m]^{\delta-}$ complex anions sit inside the framework of alkali or alkaline earth metal cations [16, 19-20]. These ternary complex hydrides are generally synthesized via reacting Ru metal and AH under pressurized hydrogen and elevated temperatures. As shown in Table 1, the crystal structure of Li_4RuH_6 or Na_4RuH_6 was determined to crystallize in the rhombohedral space group *R*-3*c*, while the $K_{2.9}RuH_{6.9}$ (~K_3RuH_7), Ca_2RuH_6 or Ba_2RuH_6 was found to crystallize in the cubic space group *Fm*-3*m*. These Ru complex hydrides, with isolated $[RuH_m]^{\delta-}$ anions linked by alkali or alkaline earth metal cations, generally have a Ru-Ru distance higher than 4.99 Å, which is distinctly different from the closely packed Ru metal surface that has Ru-Ru distance of 2.71 Å. The Bader charge analyses of these ternary Ru complex hydrides reveal that alkali or alkaline earth atoms donate their electrons to $[RuH_m]$ becoming cations, where Ru atoms exhibit a partial defective charge state and H atoms are present in a partial hydrido form [21]. Given that the bonding in the A_nRuH_m series contains a strong ionic component, these Ru complex hydrides can be classified as mixed iono-covalent bonding compounds.

Table 1. Properties of Ru complex hydrides including the space group, the lattice parameter of deuterides, the equatorial Ru-D bond distance, the Ru-Ru distance, the IR vibrational Ru-H stretching mode, the Bader's charges of Ru atom determined by AIM method, *ΔH* of

decomposition of the complex hydride (ΔH_d) via the reaction A_nRuH_m (solid) → A or AH (solid) + Ru (solid) + H_2 (gas) (see Table S1), and the corresponding decomposition temperatures (T_d). The schematic crystal structures of $Li(Na)_4RuH_6$, $Ca(Ba)_2RuH_6$ and $K_{2.9}RuH_{6.9}$ are shown above the table. The Ru, H, Li(Na), K and Ca(Ba) atoms are presented by red, yellow, light grey, light pink and light blue balls.

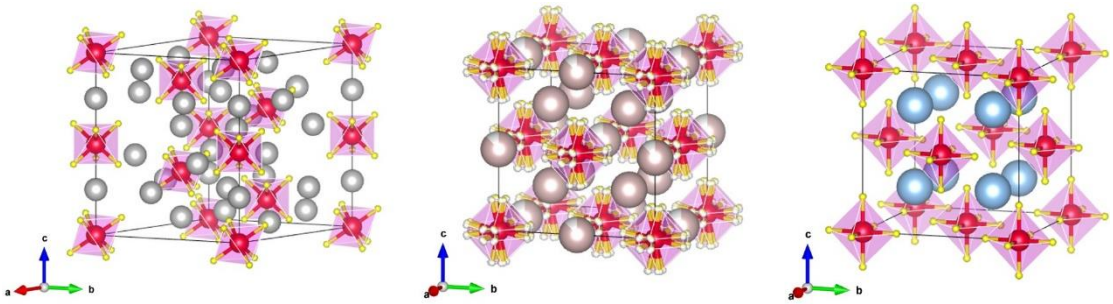

$Li(Na)_4RuH_6$ $K_{2.9}RuH_{6.9}$ $Ca(Ba)_2RuH_6$

	Space group	Lattice parameter of deuteride (a, Å)	Ru-D bond distance (Å)	Ru-Ru distance (Å)	ν(Ru-H) (cm^{-1})	Bader charge of Ru (Δq_{AIM})	ΔH_d (kJ/mol H_2)	T_d (K)
Li_4RuH_6	*R*-3*c*	8.1663	1.7144	4.9994	1527	+0.45	93.1	840
Na_4RuH_6	*R*-3*c*	9.1449	1.7912	5.6780	---	+0.26	101.9	945
$K_{2.9}RuH_{6.9}$ (~K_3RuH_7)	*Fm*-3*m*	8.4539	1.6806	5.9778	---	---	85.8	855
Ca_2RuH_6	*Fm*-3*m*	7.2214	1.7001	5.1063	1559	-0.08	175.0	1425
Ba_2RuH_6	*Fm*-3*m*	8.0166	1.7236	5.6886	1438	0.08	154.7	1305

Thermodynamic analyses show that, analogous to the previously reported Li_4RuH_6 and Ba_2RuH_6, Ca_2RuH_6, Na_4RuH_6 and K_3RuH_7 also have large enthalpy changes in hydrogen desorption, and only at high temperatures would they decompose to Ru and the corresponding A or AH (Table 1 and Table S1), which indicates that all studied Ru complex hydrides here have high thermal stabilities. Taking the facilely prepared Ca_2RuH_6 as an example, the stability of the ternary Ru complex hydride under ammonia synthesis conditions was investigated in detail. The *in situ* SR-PXD characterization reveals that the ternary hydride remains the dominant phase until 923 K under N_2+3H_2 of atmospheric pressure (Fig. 1a). The TPR-MS results show that Ca_2RuH_6 is also resistant to diluted NH_3 at temperatures below 570 K. After

introducing H_2 into the diluted NH_3, the Ca_2RuH_6 phase remains stable up to 700 K (Fig. 1b). These experimental findings demonstrate that the bulk Ca_2RuH_6 would stay stable under the ammonia synthesis conditions applied in this study (operation temperature from 473 K to 623 K, H_2 partial pressure from 0.4 to 7.5 bar).

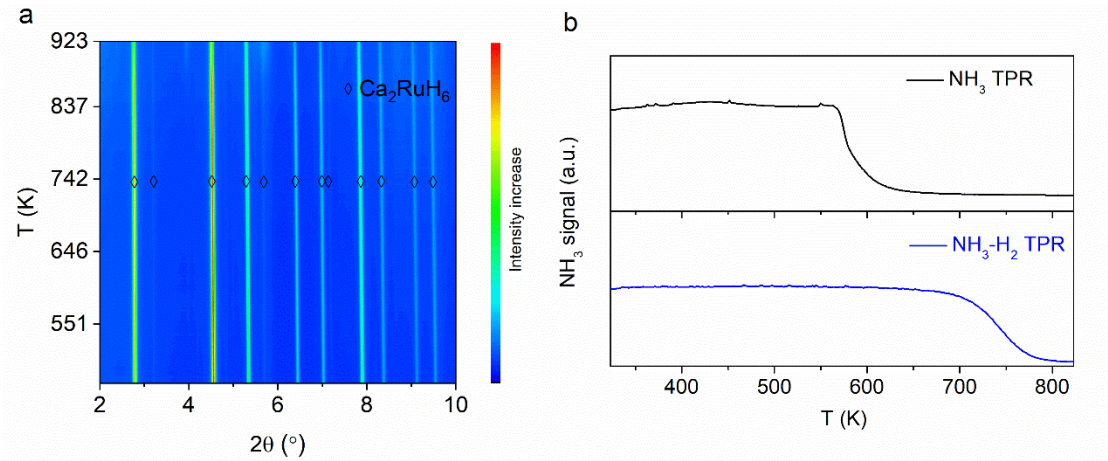

Fig. 1 a, *In situ* SR-XRD characterization of Ca_2RuH_6 sample under atmospheric N_2-$3H_2$ and elevated temperatures (from 473 K to 923 K); **b,** TPR-MS profiles of Ca_2RuH_6 in a diluted NH_3 gas (NH_3:Ar=0.5:99.5) and a diluted NH_3-H_2 mixture gas (NH_3:H_2:Ar=0.5:75:24.5).

We then performed activity test on the as-prepared bulk phase Ca_2RuH_6 sample of an average crystalline size of ca. 60 nm. As shown in Fig. 2a, the Ca_2RuH_6 sample exhibits an activity of ca. 0.4 mmol g_{Ru}^{-1} h^{-1} (or 0.22 mmol g_{cat}^{-1} h^{-1}) at 1 bar and 573 K. Cracking the Ca_2RuH_6 sample through ball-milling treatment can double its reaction rates. To further reduce its particle size as well as increase its surface area, we then ball-milled the Ca_2RuH_6 sample with inert dispersers, such as BN and MgO. As shown in Fig. S1, ball milling the Ca_2RuH_6 sample with BN and MgO can reduce the crystalline size of Ca_2RuH_6 from ca. 60 nm to ca. 25 nm and 13 nm, respectively. As expected, the ammonia synthesis rates increase gradually with the decreasing crystalline size. The as-prepared Ca_2RuH_6-BN(BM) and Ca_2RuH_6-MgO(BM) samples outperform the bulk Ca_2RuH_6 by 12 times and 57 times, respectively (Fig. 2a). We thus employed MgO as support and synthesized the supported Ca_2RuH_6/MgO catalyst. The as-prepared Ca_2RuH_6/MgO sample, with a Ru content of ca. 9.0 wt%, shows ca. 140-fold increase in activity from the bulk phase Ca_2RuH_6, but has a similar apparent activation energy of ca. 75 kJ mol^{-1} as other Ca_2RuH_6-based catalysts (Fig. 2a and fig.

S2), showing the effective exposure of ternary hydride active sites in the supported catalyst. The STEM-EDS maps of the supported sample reveal that Ca and Ru are in proximity and dispersed evenly over the MgO support (Fig. 2b). Moreover, the Ca_2RuH_6/MgO sample has a similar Ru-H stretching band (peak frequency: 1570 cm^{-1}) as that of bulk Ca_2RuH_6 sample, which is further confirmed by Ru-D stretching band (peak frequency: 1120 cm^{-1}) in the deuterated sample (Fig. 2c). The tested Ca_2RuH_6/MgO sample also exhibits similar Ru-H stretching vibration as that of bulk Ca_2RuH_6 and that of fresh Ca_2RuH_6/MgO (Fig. 2c), which demonstrates that the ternary hydride active sites remain stable under the reaction conditions.

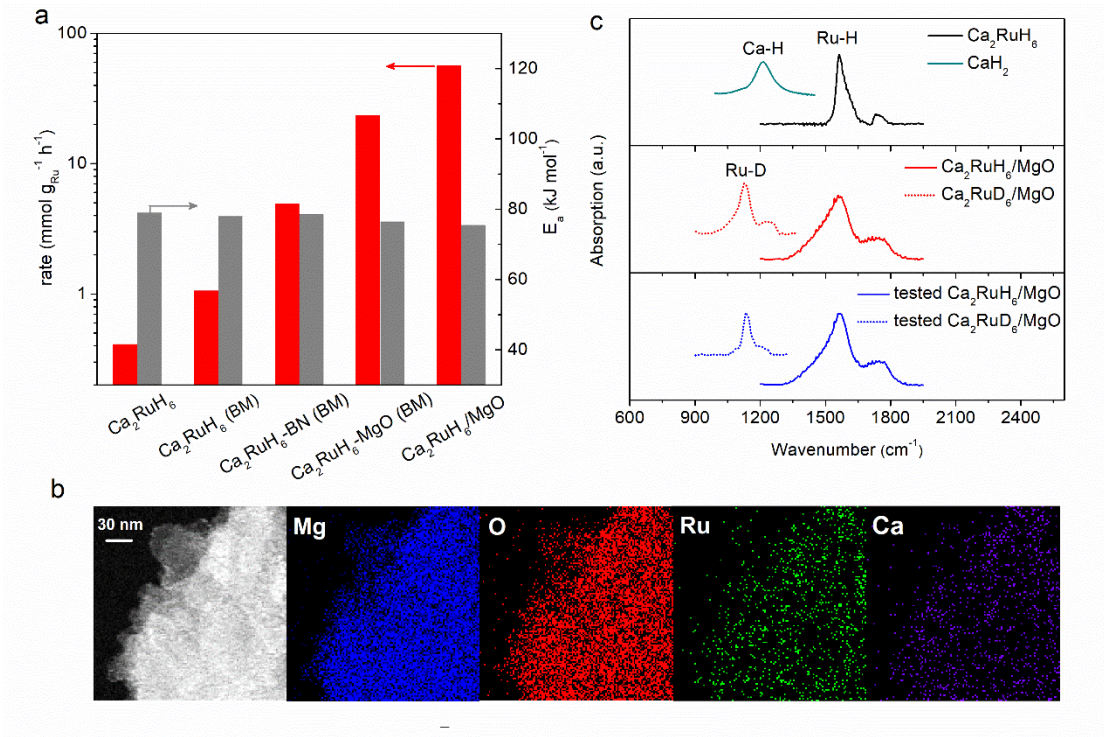

Fig. 2. a, Activities of Ca_2RuH_6-based catalysts at 573 K and the corresponding activation energies (Reaction conditions: catalyst loading 30 mg, N_2:H_2=1:3, flow rate 30 ml min^{-1}, and 1 bar); **b,** STEM and elemental mapping images of Ca_2RuH_6/MgO sample; **c,** FT-IR spectra of Ca_2RuH_6, CaH_2, $Ca_2RuH(D)_6$/MgO and tested $Ca_2RuH(D)_6$/MgO (Test conditions: N_2:$H_2(D_2)$=1:3, 20 bar and 673 K).

Following a similar approach, other supported ternary complex hydride catalysts Na_4RuH_6/MgO, K_3RuH_7/MgO were also synthesized, which possess the characteristic features of the corresponding bulk-phase ternary complex hydrides (Fig. S3). With an effective exposure of the ternary hydride active sites, these supported ternary hydride

catalysts show universal high activities, which outperform the Cs-promoted Ru catalyst (Cs-Ru/MgO), one of the most-active NH_3 synthesis catalysts, by 3-6 times at 573 K and 3-16 times at 523 K (Fig. S4). Increasing the N_2 partial pressure of the syngas can further enhance the performance of these ternary complex hydride catalysts. As shown in Fig. S5, the optimal molar ratio of N_2 and H_2 was found to be ca. 3:2. Under a N_2:H_2 ratio of 3:2 and atmospheric pressure, the K_3RuH_7/MgO catalyst exhibits higher catalytic activity than Na_4RuH_6/MgO and Ca_2RuH_6/MgO catalysts at temperatures higher than 530 K, and the NH_3 concentration formed above 593 K can reach thermodynamic equilibrium even at a space velocity as high as 60000 ml g^{-1} h^{-1}; the Ca_2RuH_6/MgO catalyst functions well at lower temperatures, which outperforms the K_3RuH_7/MgO and Na_4RuH_6/MgO catalysts by nearly an order of magnitude at 473 K (Fig. 3a). The catalytic performances of these supported ternary complex hydride catalysts got further improved as the reaction pressure increased. Comparatively, under a total pressure of 10 bar and at temperatures above 573 K, the activities of these supported Ru complex hydride catalysts are ranked in the order of K_3RuH_7/MgO ≈ Ba_2RuH_6/MgO > Li_4RuH_6/MgO > Na_4RuH_6/MgO > Ca_2RuH_6/MgO; while at temperatures below 573 K, the activity order is Ba_2RuH_6/MgO > Li_4RuH_6/MgO > Ca_2RuH_6/MgO > Na_4RuH_6/MgO > K_3RuH_7/MgO (Fig. 3b). What' more, all ternary complex hydride catalysts investigated here considerably outperform most of recently reported Ru-based catalysts especially under mild reaction conditions (Table S2). It is worth noting that if these supported ternary complex hydride samples are oxidized and deactivated in air before reaction, their activities drop significantly to the level of Ru/MgO or Cs-Ru/MgO samples (Fig. S6), which demonstrates that the ternary hydride form is of critical importance for efficient catalysis.

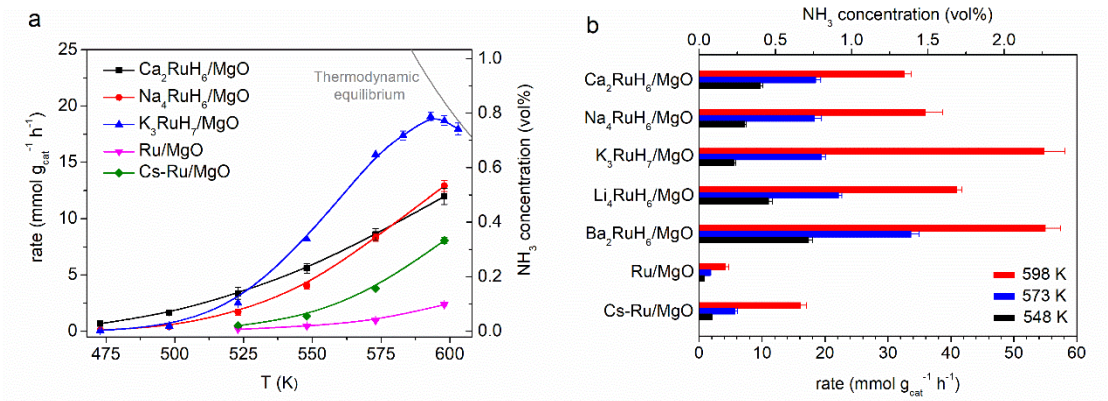

Fig. 3. a, Temperature-dependent NH_3 synthesis rates and corresponding effluent NH_3 concentration of supported ternary Ru complex hydride catalysts (Ca_2RuH_6/MgO, Na_4RuH_6/MgO and K_3RuH_7/MgO) and Ru metal based catalysts (Ru/MgO and Cs-Ru/MgO) at 1 bar (Reaction conditions: catalyst loading, 30 mg, N_2:H_2=3:2, flow rate 30 ml min^{-1}); **b,** NH_3 synthesis rates and corresponding effluent NH_3 concentration of supported ternary Ru complex hydride catalysts (Ca_2RuH_6/MgO, Na_4RuH_6/MgO, K_3RuH_7/MgO, Li_4RuH_6/MgO and Ba_2RuH_6/MgO) and Ru metal based catalysts (Ru/MgO and Cs-Ru/MgO) at 10 bar (The reaction conditions are the same as **a**).

The kinetic parameters of the supported ternary complex hydride catalysts and the reference Ru metal-based catalysts are summarized in Table 2 and Fig. S7. As we can see, the kinetic behaviors of these ternary complex hydride catalysts are closely correlated with the identity of alkali or alkaline earth cations. Generally, the Ca_2RuH_6/MgO, Li_4RuH_6/MgO or Ba_2RuH_6/MgO catalysts exhibits smaller apparent activation energies (E_a) than the Ru metal catalysts, thus enabling these ternary complex hydride catalysts particularly effective at relatively lower temperatures. While the apparent activation energies of Na_4RuH_6/MgO or K_3RuH_7/MgO catalysts are close to or even higher than that of the Ru metal catalysts, allowing them to achieve high activities at relatively higher temperatures. Moreover, the N_2 orders for all ternary complex hydride catalysts are close to 1. The Ca_2RuH_6/MgO, Li_4RuH_6/MgO or Ba_2RuH_6/MgO catalysts have positive reaction orders with respect to H_2, in clear contrast to the Ru metal based catalysts who have negative H_2 reaction orders that are close to -1, suggesting that ammonia synthesis over these ternary complex hydrides is free from hydrogen poisoning. Although the H_2 orders of Na_4RuH_6/MgO and K_3RuH_7/MgO catalysts are negative, they are still higher than that of the Ru metal based catalysts, showing a less inhibiting effect of adsorbed H on the surface of these ternary complex hydrides. The reaction orders of NH_3 for all ternary

complex hydride catalysts are negative, indicating the inhibiting effect of NH_3. Another prominent kinetic feature of this new class of ternary complex hydride catalysts is the balanced affinity towards H_2 and NH_3, i.e. when the NH_3 inhibiting effect on the ternary hydride surface gets weakened, the H_2 inhibiting effect get strengthened. Such a characteristic strikes a balance between the rates of dissociative adsorption of H_2 and the rates of associative desorption of NH_3, allowing all ternary complex hydride catalysts to exhibit superior mild-condition activities.

Table 2. Kinetic parameters of the supported ternary Ru complex hydride catalysts and reference Ru metal catalysts.

Catalyst	Reaction order[a]			Ea (kJ mol^{-1})
	α(NH_3)	β(N_2)	γ(H_2)	
Ca_2RuH_6/MgO	-0.57	0.94	0.26	75.4 (473-573 K)
Na_4RuH_6/MgO	-0.29	0.92	-0.32	115.4 (473-573 K)
K_3RuH_7/MgO	-0.36	1.17	-0.53	139.7 (473-573 K)
Li_4RuH_6/MgO	-0.59	0.91	0.30	71.2 (523-598 K)
Ba_2RuH_6/MgO	-0.63	0.92	1.00	63.9 (523-598 K)
Ru/MgO	-0.24	1.12	-0.86	94.8 (523-598 K)
Cs-Ru/MgO	-0.09	1.01	-0.82	112.4 (523-598 K)

[a]Reaction conditions: catalyst loading 30 mg, pressure 1 bar and temperature 573 K.

As reported by our previous studies [22], a different reaction mechanism towards NH_3 formation over the lithium-ruthenium ternary hydride catalyst was demonstrated, in which N_2 undergoes non-dissociative hydrogenolysis over the electron-rich [RuH_m] centers by the involvement of hydridic hydrogens in mediating electron and proton transfers and Li cations in co-stabilizing N_xH_y intermediate species. The unique configuration of the ternary complex hydride center allows all its components collaboratively involved in the catalysis, which creates an energetically more favorable pathway for N_2 activation and hydrogenation and thus endows superior

ammonia formation rates under mild conditions. Such a unique reaction mechanism might also hold true for barium/calcium/sodium/potassium-ruthenium hydride catalysts for the following reasons: 1) they share similar configurations with lithium-ruthenium hydride, where the H-rich [RuH_m] anions sit inside the framework of A cations with a Ru-Ru distance higher than 5 Å, favoring a cation-mediated non-dissociative reduction mechanism; 2) Ru in these ternary hydride compounds is in an ionic state and coordinated with multiple hydridic hydrogens, all creating an electron-rich environment for N_2 reduction. Nonetheless, the change of alkali cation still has certain effect on the electronic and structural properties of ternary complex hydride surface, which further affects its affinity towards N_2, H_2, NH_3 and some N_xH_y intermediates and hence causes changes in the macrokinetic behaviors mentioned above. We speculated that, on Li-Ru or Ca-Ru complex hydride surface, Li or Ca cations prefer to stabilizing N_2H_x (x=0, 1, 2, 3) species on [RuH_m] center, thus reducing the barrier for N_2 hydrogenation and facilitating NH_3 formation at low temperatures; on K-Ru and Na-Ru complex hydride surface, K and Na cations have more benefits for destabilizing NH_x (x=1, 2, 3) species on [RuH_m] center, thus promoting the desorption of NH_3 product and increasing the reaction rates at high temperatures or high ammonia concentration; while on Ba-Ru complex hydride surface, Ba cations help to maintain a balance between N_2 hydrogenation and NH_3 desorption over [RuH_m] center, thus enabling better performance in the whole range of test temperature.

Hydrogenolysis of N_2 to NH_3 using H_2 as the thermodynamically ideal reductant via concerted N-N weakening and N-H formation is an effective approach for mild-condition ammonia synthesis, as well as a scientific goal actively pursued in N_2 fixation for more than half a century [18]. The non-dissociative N_2 activation on a heterogeneous TM surface has been discussed before but was later found to be energetically unfavorable [23-24]. While for the well-defined TM hydride complex systems, until now only a few metallic polyhydride complexes have been reported to be capable of activating N_2 and hydrogenating it to imido/amido units, but no

ammonia was formed [25-28]. The solid-state ternary ruthenium complex hydride series presented here may serve as the first complex compound catalysts that can achieve the non-dissociative hydrogenolysis of N_2 to NH_3, which sets up a bridge linking research endeavor from heterogenous and homogeneous nitrogen fixation. Based on the understanding of the synergized scenario over ternary complex hydride active center, we propose that, in the heterogeneous catalysis regime, creating a multi-component and electron-rich catalytic center might be more favorable for non-dissociative N_2 activation and hydrogenation under mild conditions, since the dynamic and synergistic engagement of all the components may contribute to manipulating the energetics of elementary steps with multi-degree of freedom, and thus allow a reaction pathway with suitable energetics for effective hydrogenolysis of N_2 to NH_3.

Conclusion

In summary, a series of ternary ruthenium complex hydride catalysts was demonstrated to function as efficient catalysts for mild-condition ammonia synthesis, where the ternary complex hydride itself forms a powerful active center and exerts a distinct pathway to facilitate the non-dissociative N_2 reduction to NH_3. The present study not only makes a significant step towards the long-sought scientific goal, mild-condition catalytic ammonia synthesis, but also demonstrates the power of multi-component and electron-rich catalytic center to tackle the activation and conversion of inert molecules. What's more, it initiates complex hydrides as heterogeneous catalysts for the conversion of kinetically stable molecules, further unveiling the power of hydrides in catalysis.

Experimental Details

Materials and Catalyst Preparation.

Preparation of bulk ternary ruthenium complex hydride samples. Li_4RuH_6, Na_4RuH_6, K_3RuH_7, Ba_2RuH_6 and Ca_2RuH_6 samples were synthesized by the calcination of ball-milled mixtures of Ru powder (Aladdin, 99.99% metals basis) with LiH (Alfa, 99.4%), NaH (Aladdin, 90%), KH (Aladdin, 30% dispersion in mineral oil), BaH_2 and CaH_2 (Alfa, 97%) at elevated temperatures and pressures, as has been described in earlier reports [20, 29-31]. The maximum reaction pressure and temperature of our in-house built autoclaves are 50 bar and 973 K. Under the limiting conditions of the autoclave, the Na_4RuH_6 and K_3RuH_7 can only be partially synthesized, which still have a certain amount of unreacted NaH/KH and Ru. Therefore, the as-prepared Na_4RuH_6 and K_3RuH_7 in this study were denoted as Na_4RuH6* and K_3RuH_7*, respectively. BaH_2 was obtained following the procedure described previously [32].

Preparation of ball milled Ca_2RuH_6-based samples. Ca_2RuH_6 (BM), Ca_2RuH_6-BN (BM) and Ca_2RuH_6-MgO (BM) samples were prepared via ball milling Ca_2RuH_6 itself, Ca_2RuH_6 and BN (Aladdin, 98.5%, 1 μm), Ca_2RuH_6 and MgO in a H_2-filled vessel on a Retsch planetary ball mill (PM 400, Germany) at 150 r.p.m. for 3 h. The Ru content of Ca_2RuH_6-BN (BM) or Ca_2RuH_6-MgO (BM) sample is ca. 9.0 wt%. The MgO sample has a high specific surface area of ca. 534 m^2 g^{-1}, which was synthesized according to the literature report [33].

Preparation of supported Ru metal based catalysts and supported ternary ruthenium complex hydride catalysts. Two Ru/MgO catalysts with Ru contents of 8.7 wt% and 15 wt%, Cs-Ru/MgO catalyst with a Ru content of 7.3 wt%, Li_4RuH_6/MgO catalyst with a Ru content of 8.0 wt%, and Ba_2RuH_6/MgO catalyst with a Ru content of 5.0 wt% were prepared according to the procedure described in our previous report [22]. Na_4RuH_6/MgO, K_3RuH_7/MgO and Ca_2RuH_6/MgO catalysts were prepared in a similar way, except impregnating the Ru/MgO (8.7 wt% Ru/MgO for Na_4RuH_6/MgO and K_3RuH_7/MgO, 15 wt% Ru/MgO for Ca_2RuH_6/MgO) in the sodium-ammonia solution with a molar ratio of Na:Ru=4:1, potassium-ammonia

solution with a molar ratio of K:Ru=1:1, and calcium-ammonia solution with a molar ratio of Ca:Ru=6.5:1, respectively. The corresponding deuteride samples were obtained following the similar approach, except reduction in pure D_2 instead of H_2.

Characterization. Fourier transform infrared (FT-IR) measurements were conducted on a Brucker Tensor II unit with a scan resolution of 4 cm^{-1} and an accumulation of 32 scans each time. Powder X-ray diffraction (PXRD) patterns were recorded on a PANalytical X'pert diffractometer using a homemade cell covered with KAPTON film to avoid air and moisture contamination. *In situ* synchrotron radiation powder X-ray diffraction (SR-PXD) experiments were performed at the diffraction beamline P.02.1, DESY (Hamburg, Germany). The experimental procedure in detail was described in our previous study [22]. The Ca_2RuH_6 sample was heated from 298 to 923 K with a ramping rate of 6 K min^{-1} in a steam of flow gas (N_2:H_2=1:3, 5 ml min^{-1}). The 2D images were then integrated using FIT2D software. Temperature-programmed reaction (TPR) measurements were conducted in a quartz-lined stainless steel reactor and the exhaust gases were monitored with an on-line mass spectroscopy (MS, Hiden HPR20). Samples (30 mg) were heated in a stream of specific has (30 ml min^{-1}) from room temperature to desired temperatures at a ramping rate of 5 K min^{-1}. The morphology and composition of the catalyst were investigated using high angle annular dark field scanning transmission electron microscopy (HAADF-STEM, JEOL JEM-ARM200F) with an energy-dispersive X-ray spectrometer (EDX).

Catalyst activity Test. Ammonia synthesis was conducted in a stainless steel fixed-bed reaction with a quartz liner that operated with the supply of continuous-flow of extra pure N_2-H_2 mixture gas (>99.9999%). Typically, 30 mg of catalyst was loaded in the liner tube on a bed of quartz wool and subsequently heated at a ramping rate of 5 K min^{-1} under the given pressure and flow rate. The ammonia produced was trapped in a diluted sulfuric acid solution and the proton conductivity was recorded with time by a conductivity meter. The principle of the NH_3 quantification method has been described previously [34]. The activity data at each temperature was monitored when the catalytic performance reached a steady-state value. Blank test using the

same setup did not give any measurable activity at temperatures below 673 K and 10 bar.

Kinetic studies. The measurements of reaction order of N_2 or H_2 were carried out with a flow of mixed gas (N_2, H_2 and Ar) under conditions (573 K, 1 bar, WHSV=60000 ml g^{-1} h^{-1}), where the effluent NH_3 concentration was kept constant. Our measurement conditions were far from equilibrium considering that the thermodynamic limit is ca. 2.1% under these conditions. The loading amount is 30 mg for Ca_2RuH_6/MgO, Na_4RuH_6/MgO and K_3RuH_7/MgO. The gas compositions of N_2:H_2:Ar were 5:50:45, 15:50:35, 25:50:25, 35:50:15, 45:50:5 for determining the N_2 order, and 20:40:40, 20:50:30, 20:60:20, 20:80 for determining the H_2 order, respectively. The NH_3 order was determined by changing the flow rate of syngas while keeping a constant N_2 to H_2 partial pressure. Apparent activation energies were measured under atmospheric syngas (H_2:N_2=3) with a flow rate of 30 ml min^{-1}. The temperature range is 473-573 K for Ca_2RuH_6/MgO, Na_4RuH_6/MgO and K_3RuH_7/MgO.

References

1. MacFarlane, D. R.; Cherepanov, P. V.; Choi, J.; Suryanto, B. H. R.; Hodgetts, R. Y.; Bakker, J. M.; Ferrero Vallana, F. M.; Simonov, A. N., A Roadmap to the Ammonia Economy. *Joule* **2020,** *4* (6), 1186-1205.
2. Wang, Q.; Guo, J.; Chen, P., Recent progress towards mild-condition ammonia synthesis. *J. Energy Chem.* **2019,** *36*, 25-36.
3. Smith, C.; Hill, A. K.; Torrente-Murciano, L., Current and future role of Haber–Bosch ammonia in a carbon-free energy landscape. *Energy Environ. Sci.* **2020,** *13* (2), 331-344.
4. Ye, L.; Nayak-Luke, R.; Bañares-Alcántara, R.; Tsang, E., Reaction: "Green" Ammonia Production. *Chem* **2017,** *3* (5), 712-714.
5. https://royalsociety.org/topics-policy/projects/low-carbon-energy-programme/green-ammonia/. **2019**
6. Zheng, J.; Liao, F.; Wu, S.; Jones, G.; Chen, T.-Y.; Fellowes, J.; Sudmeier, T.; McPherson, I. J.; Wilkinson, I.; Tsang, S. C. E., Efficient Non-dissociative Activation of Dinitrogen to Ammonia over Lithium-Promoted Ruthenium Nanoparticles at Low Pressure. *Angew. Chem. Int. Ed.* **2019,** *58* (48), 17335-17341.
7. Vojvodic, A.; Medford, A. J.; Studt, F.; Abild-Pedersen, F.; Khan, T. S.; Bligaard, T.; Nørskov, J. K., Exploring the limits: A low-pressure, low-temperature Haber–Bosch process. *Chem. Phys. Lett.* **2014,** *598*, 108-112.
8. Kitano, M.; Inoue, Y.; Yamazaki, Y.; Hayashi, F.; Kanbara, S.; Matsuishi, S.; Yokoyama, T.;

Kim, S.-W.; Hara, M.; Hosono, H., Ammonia synthesis using a stable electride as an electron donor and reversible hydrogen store. *Nat. Chem.* **2012,** *4* (11), 934-940.
9. Tang, Y.; Kobayashi, Y.; Masuda, N.; Uchida, Y.; Okamoto, H.; Kageyama, T.; Hosokawa, S.; Loyer, F.; Mitsuhara, K.; Yamanaka, K.; Tamenori, Y.; Tassel, C.; Yamamoto, T.; Tanaka, T.; Kageyama, H., Metal-Dependent Support Effects of Oxyhydride-Supported Ru, Fe, Co Catalysts for Ammonia Synthesis. *Adv. Energy Mater.* **2018,** *8* (36), 1801772.
10. Yamashita, H.; Broux, T.; Kobayashi, Y.; Takeiri, F.; Ubukata, H.; Zhu, T.; Hayward, M. A.; Fujii, K.; Yashima, M.; Shitara, K.; Kuwabara, A.; Murakami, T.; Kageyama, H., Chemical Pressure-Induced Anion Order–Disorder Transition in LnHO Enabled by Hydride Size Flexibility. *J. Am. Chem. Soc.* **2018,** *140* (36), 11170-11173.
11. Kitano, M.; Kujirai, J.; Ogasawara, K.; Matsuishi, S.; Tada, T.; Abe, H.; Niwa, Y.; Hosono, H., Low-Temperature Synthesis of Perovskite Oxynitride-Hydrides as Ammonia Synthesis Catalysts. *J. Am. Chem. Soc.* **2019,** *141* (51), 20344-20353.
12. Inoue, Y.; Kitano, M.; Kishida, K.; Abe, H.; Niwa, Y.; Sasase, M.; Fujita, Y.; Ishikawa, H.; Yokoyama, T.; Hara, M.; Hosono, H., Efficient and Stable Ammonia Synthesis by Self-Organized Flat Ru Nanoparticles on Calcium Amide. *ACS Catal.* **2016,** *6* (11), 7577-7584.
13. Kitano, M.; Inoue, Y.; Sasase, M.; Kishida, K.; Kobayashi, Y.; Nishiyama, K.; Tada, T.; Kawamura, S.; Yokoyama, T.; Hara, M.; Hosono, H., Self-organized Ruthenium–Barium Core–Shell Nanoparticles on a Mesoporous Calcium Amide Matrix for Efficient Low-Temperature Ammonia Synthesis. *Angew. Chem. Int. Ed.* **2018,** *57* (10), 2648-2652.
14. Sato, K.; Imamura, K.; Kawano, Y.; Miyahara, S.-i.; Yamamoto, T.; Matsumura, S.; Nagaoka, K., A low-crystalline ruthenium nano-layer supported on praseodymium oxide as an active catalyst for ammonia synthesis. *Chem. Sci.* **2017,** *8* (1), 674-679.
15. Ogura, Y.; Sato, K.; Miyahara, S.-i.; Kawano, Y.; Toriyama, T.; Yamamoto, T.; Matsumura, S.; Hosokawa, S.; Nagaoka, K., Efficient ammonia synthesis over a Ru/La0.5Ce0.5O1.75 catalyst pre-reduced at high temperature. *Chem. Sci.* **2018,** *9* (8), 2230-2237.
16. K. Yvon; G. Renaudin, Hydrides: solid state transition metal complexes, John Wiley & Sons Ltd, **2006**.
17. Ballmann, J.; Munhá, R. F.; Fryzuk, M. D., The hydride route to the preparation of dinitrogen complexes. *Chem. Commun.* **2010,** *46* (7), 1013-1025.
18. Nishibayashi, Y., Nitrogen fixation (Topics in Organometallic Chemistry) **2017,** 1st edn, Vol. 60 (Springer, Heidelberg)
19. Humphries, T. D.; Sheppard, D. A.; Buckley, C. E., Recent advances in the 18-electron complex transition metal hydrides of Ni, Fe, Co and Ru. *Coord. Chem. Rev.* **2017,** *342*, 19-33.
20. Bronger, W.; Sommer, T.; Auffermann, G.; Müller, P., New alkali metal osmium- and ruthenium hydrides. *J. Alloys Compd.* **2002,** *330-332*, 536-542.
21. Orgaz, E.; Aburto, A., Electronic Structure of Ternary Ruthenium-Based Hydrides. *J. Phys. Chem. C* **2008,** *112* (39), 15586-15594.
22. Wang, Q.; Pan, J.; Guo, J.; Hansen, H. A.; Xie, H.; Jiang, L.; Hua, L.; Li, H.; Guan, Y.; Wang, P., Ternary ruthenium complex hydrides for ammonia synthesis. *ChemRxiv.* **2020,** 10.26434/chemrxiv.13465760.v1.
23. Rod, T. H.; Logadottir, A.; Nørskov, J. K., Ammonia synthesis at low temperatures. *J. of Chem. Phys.* **2000,** *112* (12), 5343-5347.
24. Garden, A. L.; Skúlason, E., The Mechanism of Industrial Ammonia Synthesis Revisited:

Calculations of the Role of the Associative Mechanism. *J. Phys. Chem. C* **2015,** *119* (47), 26554-26559.
25. Avenier, P.; Taoufik, M.; Lesage, A.; Solans-Monfort, X.; Baudouin, A.; de Mallmann, A.; Veyre, L.; Basset, J.-M.; Eisenstein, O.; Emsley, L.; Quadrelli, E. A., Dinitrogen Dissociation on an Isolated Surface Tantalum Atom. *Science* **2007,** *317* (5841), 1056-1060.
26. Shima, T.; Hu, S.; Luo, G.; Kang, X.; Luo, Y.; Hou, Z., Dinitrogen Cleavage and Hydrogenation by a Trinuclear Titanium Polyhydride Complex. *Science* **2013,** *340* (6140), 1549-1552.
27. Shima, T.; Luo, G.; Hu, S.; Luo, Y.; Hou, Z., Experimental and Computational Studies of Dinitrogen Activation and Hydrogenation at a Tetranuclear Titanium Imide/Hydride Framework. *J. Am. Chem. Soc.* **2019,** *141* (6), 2713-2720.
28. Shima, T.; Yang, J.; Luo, G.; Luo, Y.; Hou, Z., Dinitrogen Activation and Hydrogenation by C5Me4SiMe3-Ligated Di- and Trinuclear Chromium Hydride Complexes. *J. Am. Chem. Soc.* **2020,** *142* (19), 9007-9016.
29. Kritikos, M.; Nore´us, D.; Andresen, A. F.; Fischer, P., Preparation and structure of the ternary hydrides Li4RuH6, Na4RuH6, and Li4OsH6 containing octahedral transition metal hydrogen complexes. *J. Solid State Chem.* **1991,** *92* (2), 514-519.
30. Kritikos, M.; Nore´us, D., Synthesis and characterization of ternary alkaline-earth transition-metal hydrides containing octahedral [Ru(II)H6]4− and [Os(II)H6]4− complexes. *J. Solid State Chem.* **1991,** *93* (1), 256-262.
31. Moyer, R. O.; Stanitski, C.; Tanaka, J.; Kay, M. I.; Kleinberg, R., Ternary hydrides of calcium and strontium with iridium, rhodium and ruthenium. *J. Solid State Chem.* **1971,** *3* (4), 541-549.
32. Gao, W.; Wang, P.; Guo, J.; Chang, F.; He, T.; Wang, Q.; Wu, G.; Chen, P., Barium Hydride-Mediated Nitrogen Transfer and Hydrogenation for Ammonia Synthesis: A Case Study of Cobalt. *ACS Catal.* **2017,** *7* (5), 3654-3661.
33. Guan, H.; Wang, P.; Wang, H.; Zhao, B.; Zhu, Y.; Xie, Y., Preparation of Nanometer Magnesia with High Surface Area and Study on the Influencing Factors of the Preparation Process. *Acta Phys-Chim. Sin.* **2006,** *22* (7), 804-807.
34. Gao, W.; Guo, J.; Wang, P.; Wang, Q.; Chang, F.; Pei, Q.; Zhang, W.; Liu, L.; Chen, P., Production of ammonia via a chemical looping process based on metal imides as nitrogen carriers. *Nat. Energy* **2018,** *3* (12), 1067-1075.

Acknowledgements

The authors are grateful for the financial support from the National Natural Science Foundation of China (Grant Nos. 21633011, 21872137, 21922205, 21988101), Youth Innovation Promotion Association CAS (No. 2018213), DICP (DICP DCLS201701) and K. C. Wong Education Foundation (GJTD-2018-06).

Author contributions

P. C. conceived the idea and supervised the research and wrote the paper. Q.W. conducted the experimental work. J.G. supervised the experimental work. All authors

participated the discussion and data analyses.

Declaration of Interests

Authors declare no competing interest.

Supplementary Information

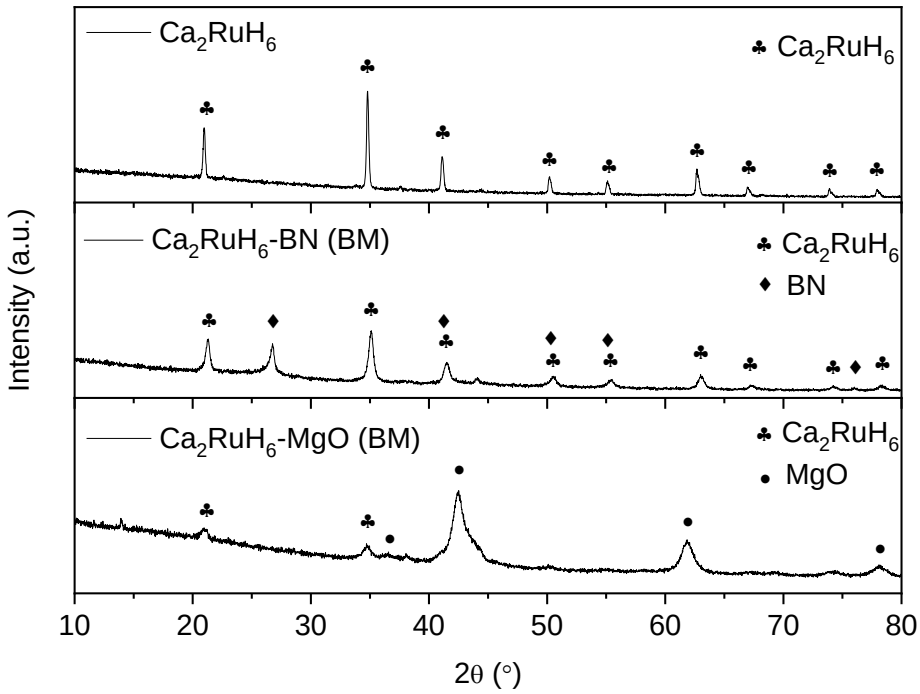

Fig. S1. XRD patterns of Ca_2RuH_6, ball-milled Ca_2RuH_6-BN sample (Ca_2RuH_6-BN (BM)) and ball-milled Ca_2RuH_6-MgO sample (Ca_2RuH_6-MgO (BM)). The crystalline sizes of Ca_2RuH_6, Ca_2RuH_6-BN (BM) and Ca_2RuH_6-MgO (BM) were estimated to be ca. 60, 25 and 13 nm, respectively, by using the Scherrer equation based on the collected XRD patterns.

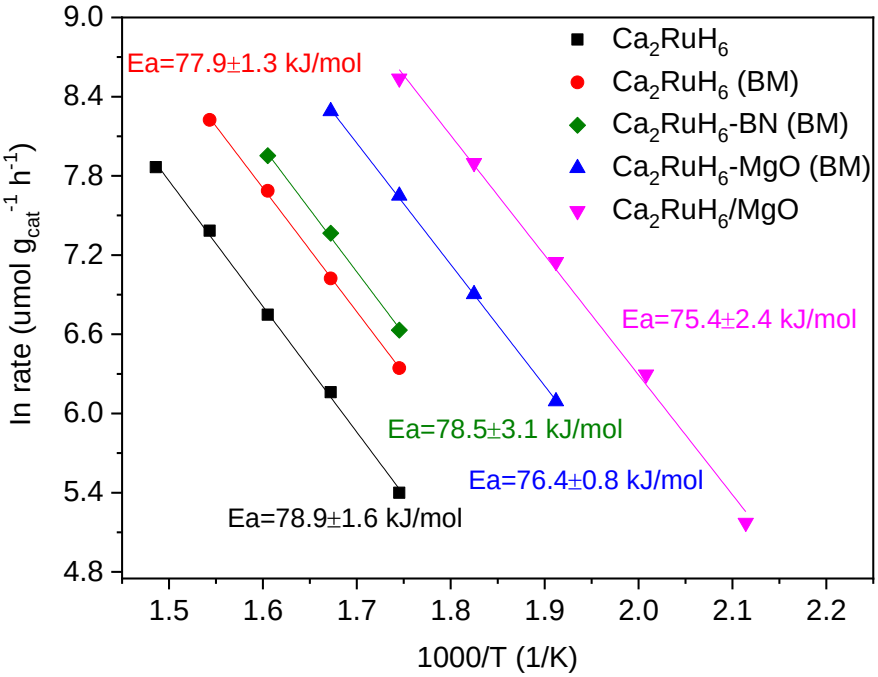

Fig. S2. Arrhenius plots of the Ca_2RuH_6, ball-milled Ca_2RuH_6 (Ca_2RuH_6 (BM)), ball-milled mixture of Ca_2RuH_6 and BN (Ca_2RuH_6-BN-(BM)), ball-milled mixture of Ca_2RuH_6 and MgO (Ca_2RuH_6-MgO-(BM)), and Ca_2RuH_6/MgO catalysts.

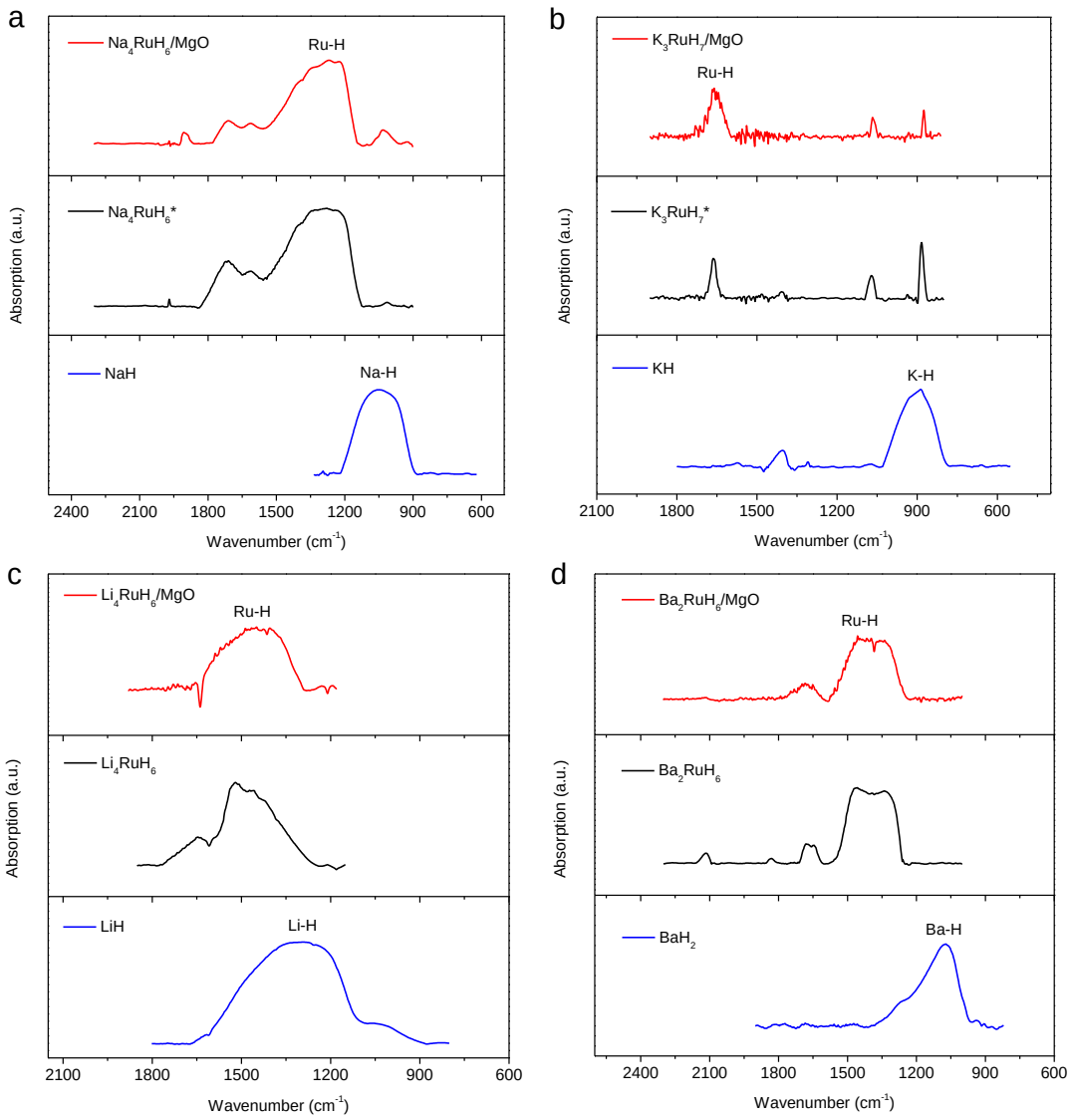

Fig. S3. a, FT-IR spectra of Na_4RuH_6/MgO, *Na_4RuH_6 and NaH; **b,** FT-IR spectra of K_3RuH_7/MgO, *K_3RuH_7 and KH; **c,** FT-IR spectra of Li_4RuH_6/MgO, Li_4RuH_6 and LiH and **d,** FT-IR spectra of Ba_2RuH_6/MgO, Ba_2RuH_6 and BaH_2. "*" indicates that the as-prepared Na_4RuH_6 and K_3RuH_7 samples are in low purity, which still have a certain amount of unreacted KH/NaH and Ru.

As shown, the Ru-H stretching bands of the as-prepared Na_4RuH_6, K_3RuH_7, Li_4RuH_6 and Ba_2RuH_6 are centered at 1280, 1660, 1500 and 1450 cm^{-1}, respectively, which are obviously distinct from A-H vibrational modes of the corresponding NaH, KH, LiH and BaH_2 reactants. The peak frequencies decrease with increasing Ru-H bond distances, which agree well with the theory-predicted results [1-2]. The IR spectra of the as-prepared supported ternary complex hydride samples show similar Ru-H stretching bands as the corresponding bulk ternary complex hydrides, indicating that the supported ternary complex hydrides have been successfully synthesized.

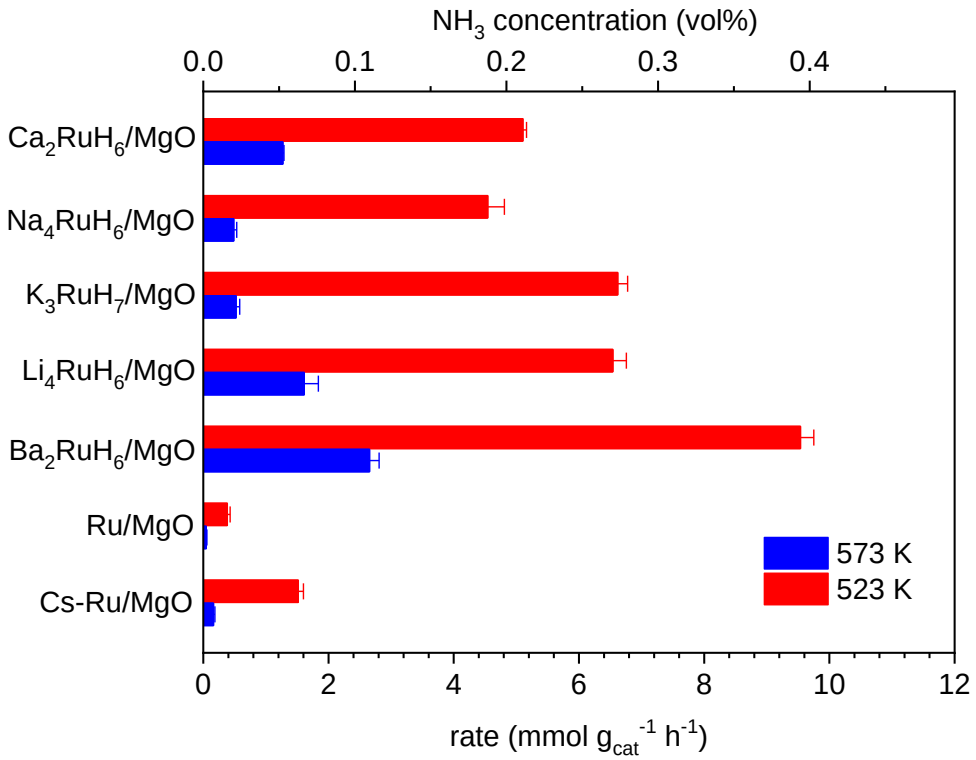

Fig. S4. NH_3 synthesis rates and corresponding effluent NH_3 concentration of supported ternary Ru complex hydride catalysts (Ca_2RuH_6/MgO, Na_4RuH_6/MgO, K_3RuH_7/MgO, Li_4RuH_6/MgO and Ba_2RuH_6/MgO) and Ru metal based catalysts (Ru/MgO and Cs-Ru/MgO) at 1 bar (Reaction conditions: catalyst loading 30 mg, N_2:H_2=1:3, flow rate 30 ml min^{-1}).

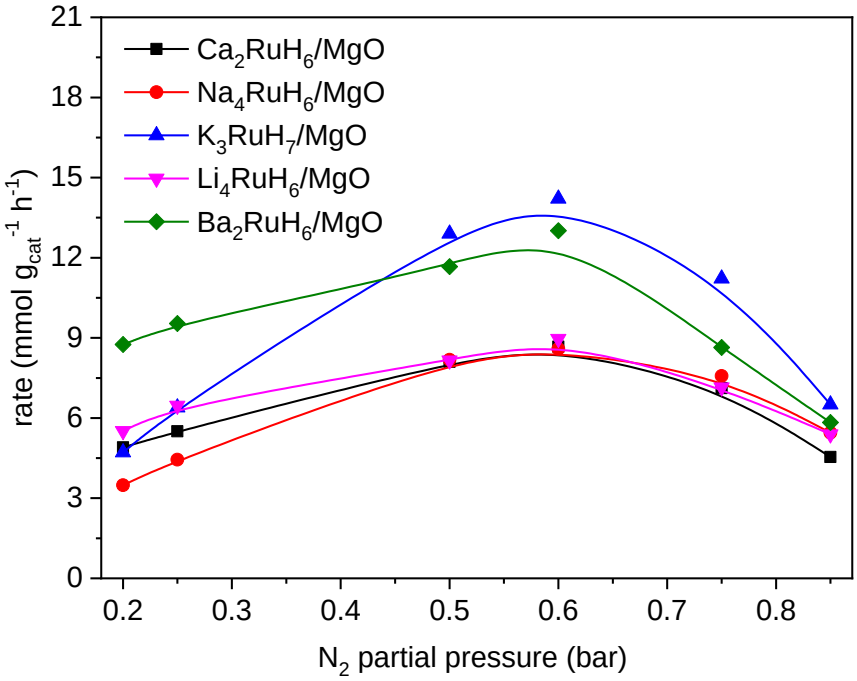

Fig. S5. NH_3 synthesis rates of supported ternary Ru complex hydride catalysts as a function of N_2 partial pressure (Reaction conditions: catalyst loading 30 mg, flow rate 30 ml min^{-1}, 573 K, and the total pressure of N_2-H_2 mixture gas is 1 bar.)

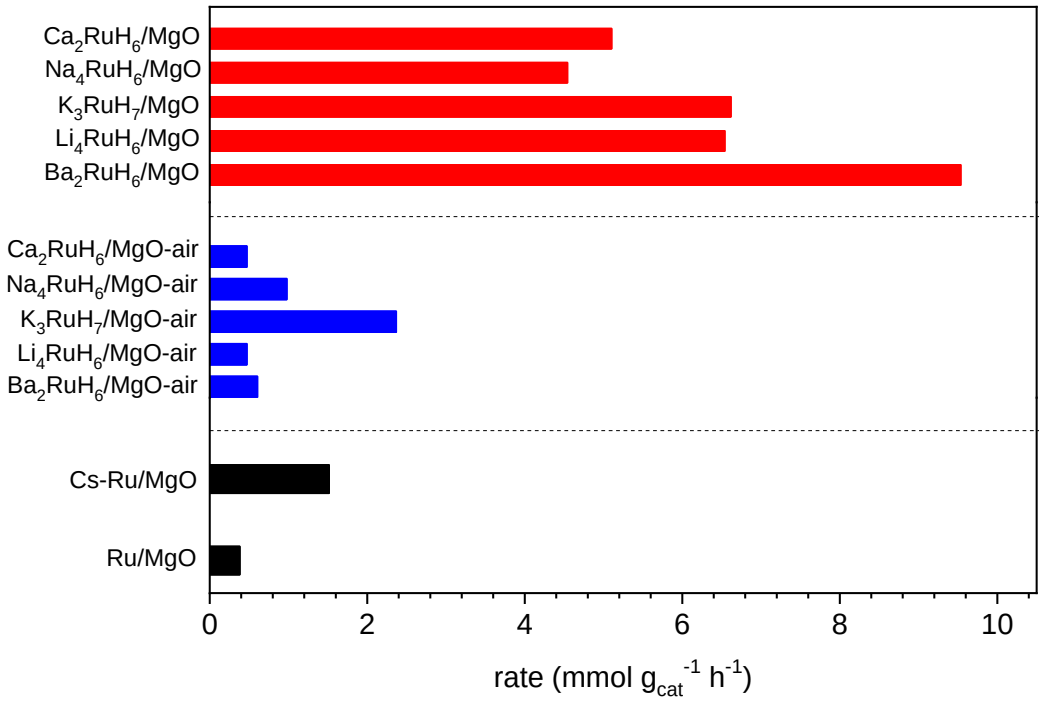

Fig. S6. NH_3 synthesis rates of Ca_2RuH_6/MgO, Na_4RuH_6/MgO, K_3RuH_7/MgO, Li_4RuH_6/MgO, Ba_2RuH_6/MgO, Ca_2RuH_6/MgO-air, Na_4RuH_6/MgO-air, K_3RuH_7/MgO-air, Li_4RuH_6/MgO-air, Ba_2RuH_6/MgO-air, Cs-Ru/MgO and Ru/MgO catalysts at 573 K (Reaction conditions: catalyst loading 30 mg, flow rate 30 ml min^{-1}, N_2:H_2=1:3, and 1 bar).

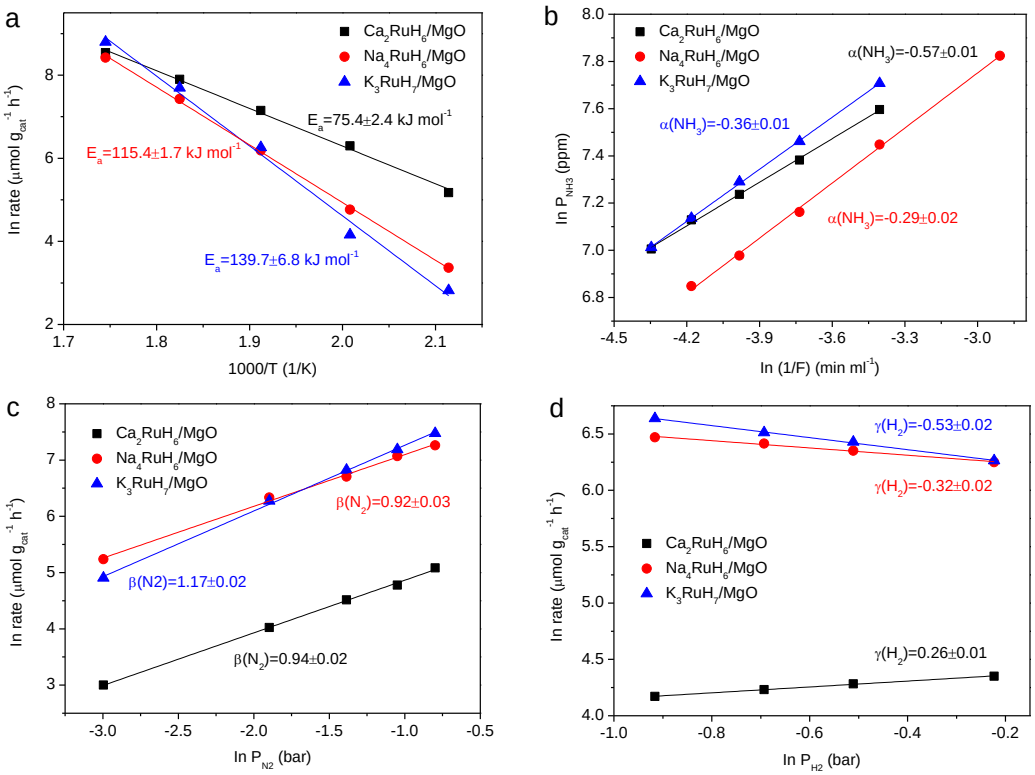

Fig. S7. a, Arrhenius plots of Ca_2RuH_6/MgO, Na_4RuH_6/MgO and K_3RuH_7/MgO catalysts; **b** to **d** Dependence of ammonia synthesis rates on the partial pressures of NH_3, N_2 and H_2, respectively, under a total pressure of 1 bar at 573 K over Ca_2RuH_6/MgO, Na_4RuH_6/MgO and K_3RuH_7/MgO catalysts.

Table S1. Thermodynamic calculations for the decomposition reactions of ternary ruthenium complex hydrides. The reaction enthalpy of Li_4RuH_6 decomposition ($\Delta_rH^0(Li_4RuH_6)$) was obtained following the pressure-composition-isotherm measurements described previously [3]. The reaction enthalpies of other ternary ruthenium complex hydrides decomposition are taken from Ref. [4] and Ref. [5]. The standard enthalpies of formation of other substances are taken from "NIST Standard Reference Number 69". Therefore, the standard enthalpies of formation of ternary ruthenium complex hydrides can be evaluated by combining the Δ_rH^0 and Δ_fH^0 values.

Reaction	Li_4RuH_6	→	4LiH	+	Ru	+	H_2	Δ_rH^0 (kJ mol^{-1})
Δ_fH^0 (kJ mol^{-1})	-455.1		-90.5		0		0	93.1
Reaction	$1/3Na_4RuH_6$	→	4/3Na	+	1/3Ru	+	H_2	Δ_rH^0 (kJ mol^{-1})
Δ_fH^0 (kJ mol^{-1})	-305.7		0		0		0	101.9
Reaction	$1/3Ba_2RuH_6$	→	2/3Ba	+	1/3Ru	+	H_2	Δ_rH^0 (kJ mol^{-1})
Δ_fH^0 (kJ mol^{-1})	-464.1		0		0		0	154.7
Reaction	$1/3Ca_2RuH_6$	→	2/3Ca	+	1/3Ru	+	H_2	Δ_rH^0 (kJ mol^{-1})
Δ_fH^0 (kJ mol^{-1})	-525.0		0		0		0	175.0
Reaction	$2/7K_3RuH_7$	→	6/7K	+	2/7Ru	+	H_2	Δ_rH^0 (kJ mol^{-1})
Δ_fH^0 (kJ mol^{-1})	-300.3		0		0		0	85.8

Table S2. Ammonia synthesis over recently developed Ru-based catalysts.

Catalysts	Metal content (wt %)	r_{NH3}[a] (mmol g_{Ru}^{-1} h^{-1})		WHSV (ml g^{-1} h^{-1})	Ref.
		573 K, 10 bar	573 K, 1 bar		
Ca_2RuH_6/MgO	9.0	206	96	60000	this work
Na_4RuH_6/MgO	7.6	241	109	60000	
K_3RuH_7/MgO	8.2	237	191	60000	
Li_4RuH_6/MgO	8.0	275	114	60000	
Ba_2RuH_6/MgO	5.0	673	276	60000	
Ru/$C_{12}A_7$:e^-	1.8	94 (593 K)	41	36000	6
Ru/Ca_2N:e^-	1.8	228 (593 K)	93	36000	6
Ru/$BaTiO_{2.5}H_{0.5}$	2.5	---	19 (598 K)	66000	7
Ru/$Ca(NH_2)_2$	10	158 (8 bar)	56	36000	8
Ru/Ba-$Ca(NH_2)_2$	10	233 (9 bar)	90	36000	9
Ru/Pr_2O_3	5	18 (9 bar)	---	18000	10
Ru/$La_{0.5}Ce_{0.5}O_{1.75}$	5	22	---	72000	11
Ru/BaO-CaH_2	10	165 (9 bar)	69	36000	12
Ru/$BaCeO_{3-x}N_yH_z$	4.5	111 (9 bar)	---	36000	13
Ba-Ru-Li/AC	4.8	---	1.5	62400	14
LaRuSi	37.7	---	4.7 (673 K)	36000	15

[a]Ammonia synthesis rates per gram of Ru under 573 K, 10 bar and 573 K, 1bar (H_2:N_2=3 or 2/3), unless otherwise stated.

References

1. Humphries, T. D.; Sheppard, D. A.; Buckley, C. E., Recent advances in the 18-electron complex transition metal hydrides of Ni, Fe, Co and Ru. *Coord. Chem. Rev.* **2017,** *342*, 19-33.

2. Bronger, W.; Sommer, T.; Auffermann, G.; Müller, P., New alkali metal osmium- and ruthenium hydrides. *J. Alloys Compd.* **2002,** *330-332*, 536-542.

3. Wang, Q.; Pan, J.; Guo, J.; Hansen, H. A.; Xie, H.; Jiang, L.; Hua, L.; Li, H.; Guan, Y.; Wang, P., Ternary ruthenium complex hydrides for ammonia synthesis. *ChemRxiv.* **2020,** 10.26434/chemrxiv.13465760.v1.

4. Nicholson, K. M.; Sholl, D. S., First-Principles Screening of Complex Transition Metal Hydrides for High Temperature Applications. *Inorg. Chem.* **2014,** *53* (22), 11833-11848.

5. Nicholson, K. M.; Sholl, D. S., First-Principles Prediction of New Complex Transition Metal Hydrides for High Temperature Applications. *Inorg. Chem.* **2014,** *53* (22), 11849-11860.

6. Kitano, M.; Inoue, Y.; Ishikawa, H.; Yamagata, K.; Nakao, T.; Tada, T.; Matsuishi, S.; Yokoyama, T.; Hara, M.; Hosono, H., Essential role of hydride ion in ruthenium-based ammonia synthesis catalysts. *Chem. Sci.* **2016,** *7* (7), 4036-4043.

7. Tang, Y.; Kobayashi, Y.; Masuda, N.; Uchida, Y.; Okamoto, H.; Kageyama, T.; Hosokawa, S.; Loyer, F.; Mitsuhara, K.; Yamanaka, K.; Tamenori, Y.; Tassel, C.; Yamamoto, T.; Tanaka, T.; Kageyama, H., Metal-Dependent Support Effects of Oxyhydride-Supported Ru, Fe, Co Catalysts for Ammonia Synthesis. *Adv. Energy Mater.* **2018,** *8* (36), 1801772.

8. Inoue, Y.; Kitano, M.; Kishida, K.; Abe, H.; Niwa, Y.; Sasase, M.; Fujita, Y.; Ishikawa, H.; Yokoyama, T.; Hara, M.; Hosono, H., Efficient and Stable Ammonia Synthesis by Self-Organized Flat Ru Nanoparticles on Calcium Amide. *ACS Catal.* **2016,** *6* (11), 7577-7584.

9. Kitano, M.; Inoue, Y.; Sasase, M.; Kishida, K.; Kobayashi, Y.; Nishiyama, K.; Tada, T.; Kawamura, S.; Yokoyama, T.; Hara, M.; Hosono, H., Self-organized Ruthenium–Barium Core–Shell Nanoparticles on a Mesoporous Calcium Amide Matrix for Efficient Low-Temperature Ammonia Synthesis. *Angew. Chem. Int. Ed.* **2018,** *57* (10), 2648-2652.

10. Sato, K.; Imamura, K.; Kawano, Y.; Miyahara, S.-i.; Yamamoto, T.; Matsumura, S.; Nagaoka, K., A low-crystalline ruthenium nano-layer supported on praseodymium oxide as an active catalyst for ammonia synthesis. *Chem. Sci.* **2017,** *8* (1), 674-679.

11. Ogura, Y.; Sato, K.; Miyahara, S.-i.; Kawano, Y.; Toriyama, T.; Yamamoto, T.; Matsumura, S.; Hosokawa, S.; Nagaoka, K., Efficient ammonia synthesis over a Ru/La0.5Ce0.5O1.75 catalyst pre-reduced at high temperature. *Chem. Sci.* **2018,** *9* (8), 2230-2237.

12. Hattori, M.; Mori, T.; Arai, T.; Inoue, Y.; Sasase, M.; Tada, T.; Kitano, M.; Yokoyama, T.; Hara, M.; Hosono, H., Enhanced Catalytic Ammonia Synthesis with Transformed BaO. *ACS Catal.* **2018,** *8* (12), 10977-10984.

13. Kitano, M.; Kujirai, J.; Ogasawara, K.; Matsuishi, S.; Tada, T.; Abe, H.; Niwa, Y.; Hosono, H., Low-Temperature Synthesis of Perovskite Oxynitride-Hydrides as Ammonia Synthesis Catalysts. *J. Am. Chem. Soc.* **2019,** *141* (51), 20344-20353.

14. Zheng, J.; Liao, F.; Wu, S.; Jones, G.; Chen, T.-Y.; Fellowes, J.; Sudmeier, T.; McPherson, I. J.; Wilkinson, I.; Tsang, S. C. E., Efficient Non-dissociative Activation of Dinitrogen to Ammonia over Lithium-Promoted Ruthenium Nanoparticles at Low Pressure. *Angew. Chem. Int. Ed.* **2019,** *58* (48), 17335-17341.

15. Wu, J.; Li, J.; Gong, Y.; Kitano, M.; Inoshita, T.; Hosono, H., Intermetallic Electride Catalyst

as a Platform for Ammonia Synthesis. *Angew. Chem. Int. Ed.* **2019,** *58* (3), 825-829.